



HAL
open science

Behaviour of P, Si, Ni impurities and Cr in self ion irradiated Fe–Cr alloys – Comparison to neutron irradiation

Cristelle Pareige, V. Kuksenko, Philippe Pareige

► **To cite this version:**

Cristelle Pareige, V. Kuksenko, Philippe Pareige. Behaviour of P, Si, Ni impurities and Cr in self ion irradiated Fe–Cr alloys – Comparison to neutron irradiation. *Journal of Nuclear Materials*, 2015, 456, pp.471-476. 10.1016/j.jnucmat.2014.10.024 . hal-02061876

HAL Id: hal-02061876

<https://hal.science/hal-02061876>

Submitted on 29 May 2019

HAL is a multi-disciplinary open access archive for the deposit and dissemination of scientific research documents, whether they are published or not. The documents may come from teaching and research institutions in France or abroad, or from public or private research centers.

L'archive ouverte pluridisciplinaire **HAL**, est destinée au dépôt et à la diffusion de documents scientifiques de niveau recherche, publiés ou non, émanant des établissements d'enseignement et de recherche français ou étrangers, des laboratoires publics ou privés.

Behaviour of P, Si, Ni impurities and Cr in self ion irradiated Fe–Cr alloys – Comparison to neutron irradiation

C. Pareige*, V. Kuksenko, P. Pareige

Groupe de Physique des Matériaux, Université et INSA de Rouen, UMR 6634 CNRS Avenue de l'Université, BP 12, 76801 Saint Etienne du Rouvray, France

A B S T R A C T

This paper presents an atom probe tomography study of phase transformation and solute segregation in Fe–Cr alloys of low purity under self-ion irradiation. Fe–9%Cr and Fe–12%Cr were irradiated at 100 °C, 300 °C and 420 °C at a dose of 0.5 dpa. Homogeneously distributed clusters enriched in Cr, P, Si and Ni are shown to form at 300 °C and 420 °C but not at 100 °C. Study of the evolution of the segregation intensities of Cr, Si and P in the clusters with temperature under ion irradiation indicates that they form by a radiation induced mechanism. No α' clusters were observed whatever the irradiation temperature whereas they were observed in the same alloys after neutron irradiation at 300 °C at 0.6 dpa. Comparison of the solute cluster composition after ion irradiation and neutron irradiation, suggests that P atoms could play an important role in the appearance of the solute clusters by stabilizing point defect clusters that could later be enriched in Ni, Si and Cr.

1. Introduction

Ferritic–martensitic (F–M) steels with a high chromium content (7–12%) are promising candidates as structural materials in Gen-IV reactors (for fuel assemblies, core support/internals...) because of their low ductile–brittle transition temperature (DBTT) shift, low swelling and reduced creep rate [1,2] under 600 °C. The understanding of the role of the different alloying elements and impurities on the evolution of the microstructure of F–M steels under working conditions is a key point in order to be able to predict their behaviour after long term ageing and irradiation. Investigation of irradiated F–M steels showed the formation of phases that are susceptible to alter the mechanical properties of the steels. These phases are α' phase [3–5], G-phase [2,5,6], χ phase [4,5], M_6C [3,6], σ phase [2,6,7] and laves phases [2]. Recent investigation at the atomic scale performed by Jiao et al. [8,9] revealed also the formation of other second phase particles as Ni/Si/Mn-rich precipitates, Cu-rich precipitates and Cr-rich precipitates.

Because the microstructure evolution under irradiation of the steels is very complex and because it is important to understand the role of the different elements and the possible synergies, studies focussed on the evolution of the microstructure of some Fe–Cr model alloys with different Cr contents (2.5%, 5%, 9% and 12%) and with P, Si and Ni at impurity levels were performed in the framework of the European project GETMAT [10]. The investigation of

the four model alloys of low purity after neutron irradiation with Atom Probe Tomography (APT) and Small Angle Neutron Scattering (SANS) [11,12] confirmed the radiation enhanced nature of the α' precipitation [3]. The recent work of Bachhav et al. [13] also agrees on that. APT investigations also highlighted that, under neutron irradiation at 300 °C at 0.6 dpa, Si, P and Ni that are at impurity levels participate to the formation of solute clusters enriched in Cr, Si, P and Ni [11,14]. The very low nominal levels of Ni, P and Si in the alloys totally exclude any thermodynamic driving force for precipitation process. From results in [11,14], it was concluded that the Cr/Si/P/Ni clusters have a radiation induced origin. The Cr/Si/P/Ni clusters are possibly related to the precipitates observed in irradiated steels. It is also worth noting that Ni and Si are also involved in the formation of radiation induced nano clusters in the bainitic matrix of pressure vessel steels (in association to copper and manganese [15–17]).

In order to confirm the radiation induced nature of the Cr/Si/P/Ni clusters, investigation of temperature dependant irradiations were undertaken. It was performed through self-ion irradiations undertaken at 100 °C, 300 °C and 420 °C at 0.5 dpa on the Fe–9%Cr and Fe–12%Cr alloys as described in the first part of the paper. Based on APT characterization of the clusters formed, we conclude, in the second part of the paper, on the induced nature of the solute clusters. In the last part, the microstructure after ion irradiation is compared to the one observed after neutron irradiation [11,14]. The differences and commonalities between the microstructures observed in the two cases are discussed.

E-mail address: cristelle.pareige@univ-rouen.fr (C. Pareige).

2. Materials and technique

2.1. Materials

Fe–9%Cr and Fe–12%Cr model alloys were fabricated at the University of Ghent (Belgium) by furnace melting of industrial purity Fe and Cr [18,19]. They were delivered by SCK-CEN, Mol, Belgium in the framework of the European GETMAT project [20]. After casting, the ingots were cold worked under protective atmosphere to produce 9 mm thick plates. Alloys were then heat treated at 1050 °C for 3 h in high vacuum for austenization and stabilization. Thereafter, tempering was performed at 730 °C for 4 h, followed by air cooling. The chemical composition of the model alloys measured using induced coupled plasma mass spectrometry [18,19] and APT are reported in Table 1. All the compositions reported in this work are quoted in atomic percent. Note that APT investigations of the pre-irradiated alloys did not reveal any intra-granular segregation or precipitation before irradiation [11,14].

2.2. Irradiation conditions

Massive samples ($10 \times 10 \times 1 \text{ mm}^3$) were firstly mirror polished mechanically and then electro-chemically polished in a solution of 2% of perchloric acid and 98% of ethylene glycol monobutyl ($T = 0\text{--}20 \text{ }^\circ\text{C}$, $V \approx 75 \text{ V}$) in order to remove plastic deformation introduced during mechanical polishing. They were irradiated with Fe^+ ions of 0.5 MeV, 2 MeV and 5 MeV in the Ion Beam Center in HZDR through the SPIRIT Transnational Access Platform. The use of these three energies enabled to obtain a quasi-constant damage up to $1.5 \text{ }\mu\text{m}$ as calculated with SRIM (Stopping and Range of Ions in Matter) [21,22]. A displacement threshold of 40 eV [23] was used for the calculations. The ion flux was $2 \times 10^{15} \text{ ions/m}^2/\text{s}$ and the calculated dose using the “Quick” Kinchin and Pease option as recommended by Stoller et al. [24] is 0.5 dpa. The Fe–9%Cr was irradiated at 100 °C, 300 °C and 420 °C. The Fe–12%Cr alloy was irradiated at 300 °C.

The results obtained in self-irradiated alloys will be compared to those obtained in the same alloys after neutron irradiation in the BR2 reactor. Irradiation were performed in the framework of the MIRE-Cr irradiation program at 300 °C with a neutron flux of $9 \times 10^{13} \text{ n}/(\text{cm}^2\text{s})$ ($E > 1 \text{ MeV}$) at 0.6 NRT dpa [25]. Information on irradiation conditions, mechanical properties and TEM characterization can be found in Ref. [18,19]. Characterization of irradiation damage and microstructural evolution of these alloys are already published elsewhere: SANS [12,26,27], Positron Annihilation Spectroscopy (PAS) [28], nano-indentation [29] and APT [11,14,30,31].

2.3. Atom probe technique

The samples were studied by means of an Energy Compensated Wide-Angle Tomographic Atom Probe (ECoWATAP). This instrument is equipped with an advanced delay line position-sensitive detector (aDL) which minimizes the loss of information due to impact superposition or multi-event detection [32]. The detector

efficiency is 50%. The energy compensated lens provides to ECoWATAP a high mass resolution and improves the accuracy of composition measurements [33,34].

During experiments, the specimens were cooled down to a temperature of 45–50 K in order to mitigate the preferential field evaporation process of chromium atoms. The specimens were electrically pulsed with a pulse fraction of 20% and a pulse rate equal to 30 kHz. The basic principle of APT technique may be found in different books or reviews [34–36].

APT samples were lifted out using a dual FIB-SEM (Zeiss NVISION 40) at a depth of about 500–700 nm from the surface of the samples in order to analyze an irradiated zone that is not affected by surface effects. This roughly corresponds to the position of the peak damage of the 2 MeV Fe^+ ions. The final milling was performed with a Ga beam energy of 2 kV in order to avoid implantation of Ga ions in the material.

As APT measurements are very local and as studied alloys exhibit a martensitic structure with a non-homogeneous distribution of defect sinks, 3–6 different APT samples were investigated for each ageing condition. No significant disparities in the results (in terms of number density, size, composition of features) have been observed.

3D reconstructions and data processing were performed using the 3D Data Software for Atom Probe users developed by the group of research GPM in Rouen (see authors affiliation). As far as the measurement of the size and the number density of clusters are concerned, a data filter in composition was used. The filter, called “Iso position”, enables to distinguish the particles from the surrounding matrix owing to their composition [37]. It runs in two steps. In the first step, the goal is to identify the atoms which belong to clusters. To do so, the analyzed volume is laid out in a grid pattern of cubes. The concentration of the selected chemical specie A is measured in each cube. Afterwards, a value of the concentration of A is attributed to each atom of the cube. This value is obtained by linear interpolation between the value of the concentration of A in the cube and in its neighbor cubes. If the concentration of A is higher than the chosen threshold, the atom is considered as belonging to a cluster; else it is associated to the matrix. In the second step, only the atoms belonging to clusters are taken into account. The goal, at this stage, is to distinguish all the clusters from the others. To achieve this goal, a separation distance d is chosen. All atoms labeled “clusters” situated closer than d to each other pertain to the same cluster. Finally, only clusters containing more than N_{min} atoms are considered as clusters. In this study, we chose cubes of 1.5 nm size for the grid pattern, $d = 0.2 \text{ nm}$ and $N_{\text{min}} = 130$ atoms. The choice of these parameters enables to select all the Cr/Si/P/Ni clusters visible in the analyzed volume and to distinguish them from the concentration fluctuations in the matrix.

We have shown in previous works [11,14,30,31] that two families of clusters and particles can be observed after neutron irradiation in these alloys: α' particles and NiSiPCr-enriched clusters. But, as it will be seen below, only NiSiPCr-enriched clusters were observed after ion irradiation. Consequently, only a concentration

Table 1
Nominal chemical composition (at.%) of model alloys as measured by ICP-MS (from [18,19]) and APT.

Alloy	Technique	Fe	Cr	Si	P	Ni	Mn	V	C	N	O	S	Al	Ti
Fe–9%Cr	ICP-MS	Bal.	8.93	0.18	0.02	0.07	0.03	0.002	0.09	0.06	0.23	0.001	0.014	0.004
	APT	Bal.	9.16 ± 0.04	0.065 ± 0.003	0.013 ± 0.001	0.057 ± 0.003	N.M.*	N.M.	N.M.	N.M.	N.M.	N.M.	N.M.	N.M.
Fe–12%Cr	ICP-MS	Bal.	12.33	0.22	0.09	0.085	0.03	0.002	0.129	0.09	0.22	0.012	0.006	0.004
	APT	Bal.	11.2 ± 0.04	0.18 ± 0.01	0.025 ± 0.002	0.07 ± 0.01	N.M.	N.M.	N.M.	N.M.	N.M.	N.M.	N.M.	N.M.

* N.M. not measurable.

threshold on impurity concentration was used for data treatment of ion irradiated samples: $(X_{Si} + X_{Ni} + X_P) > 1.2$ at.%. Values used for the data treatment of neutron irradiated samples are given in [11,14,30,31].

Radius of the clusters are given by the Guinier Radius i.e. $R = \sqrt{\frac{2}{3}}R_g$ where R_g is the radius of gyration. Radius of gyration is calculated from the position of the impurity atoms only (Ni, Si and P).

Concerning the composition of the clusters, the values were averaged over all the measurements performed in the core of each cluster (between 30 and 85 clusters) i.e. the values do not depend on the threshold value. The uncertainty on the composition is given by two standard deviation [34–36] $(2\sigma = 2 \times (C(1 - C)/N)^{1/2}$ where C is the atomic concentration and N the number of collected atoms).

3. Results and discussion

3.1. Microstructure after ion irradiation

Fig. 1 presents the 3D distributions of Si and P atoms in the Fe–9%Cr irradiated at 100 °C, 300 °C and 420 °C at 0.5 dpa. Fig. 2a presents the 3D distributions of the same species in the Fe–12%Cr irradiated at 300 °C at the same dose.

3.1.1. Irradiation at 300 °C of the Fe–9%Cr and Fe–12%Cr alloys

Clusters enriched by Si and P are visible in the two alloys but no α' clusters. The clusters are homogeneously distributed. The number density and radius of the clusters are given in Table 2. They are similar in the two alloys. In addition to P and Si, these clusters are also enriched in Ni and Cr. Table 3 gives the solute enrichment of the species in the clusters – $\Delta C_i = C_i - C_i^{matrix}$ – where C_i is the measured core concentration of the specie i . According to these data, clusters present the same Si and Ni enrichment. For Cr and P, the situation is less clear. A slightly lower Cr enrichment is observed in the Fe–12%Cr. A slightly higher P enrichment is measured in the Fe–12%Cr which presents a higher nominal level in P. But because of the large uncertainties (see Table 3), it is not possible to be sure that these differences are significant. So, as Cr and P

enrichment variations with the alloy composition cannot be firmly established, we will consider that there is no dependence of solute and impurity enrichments of the clusters on the composition of the alloys.

3.1.2. Irradiation of the Fe–9%Cr at 100 °C, 300 °C and 420 °C

The Fe–9%Cr was also irradiated at 100 °C and 420 °C (Fig. 1). There are no clusters in the analyzed volume after ion irradiation at 100 °C. At 420 °C, solute-enriched clusters are observed. Fig. 1 also displays segregation of Si and P atoms at dislocation lines. Composition measurements along the dislocation lines reveal also Cr enrichment. There is still no α' precipitates.

The composition of the clusters, their size and number density are provided in Fig. 3 and in Table 2. At 420 °C, clusters are bigger than they are at 300 °C with a lower number density. Their solute content is higher at 420 °C than at 300 °C. The total solute enrichment reaches 15.7 at.% at 420 °C versus 10.6 at.% at 300 °C. The increase in solute concentration is mainly related to the increase in P and Cr content (Fig 3).

Evolution of the element enrichment with temperature is presented for Cr, Si and P in Fig. 4. For P and Cr, the intensity of segregation increases when temperature increases. For Si, a decrease is observed after 300 °C. The trend has to be confirmed by complementary investigations made at higher temperature.

The segregation behavior of the different elements is fully coherent with the left part of the bell-shaped temperature dependence expected for radiation induced segregation (RIS). At 100 °C, the low mobility of the point defects and their high creation rate involves the increase in recombination rate of point defects and in formation of defects clusters when defects of the same nature meet. The latter was confirmed by positron annihilation spectroscopy (PAS) [38,39] undertaken on the same alloys. Doppler broadening PAS revealed the presence of vacancy clusters at 100 °C that were not observed at higher temperature. Consequently, because fewer point defects participate to diffusion of elements and because to their very low thermal mobility, there is no diffusion towards the sinks and thus no RIS is observed. When temperature increases, diffusion of impurities and of solute atoms is more efficient because of the higher mobility of point defects and the lower

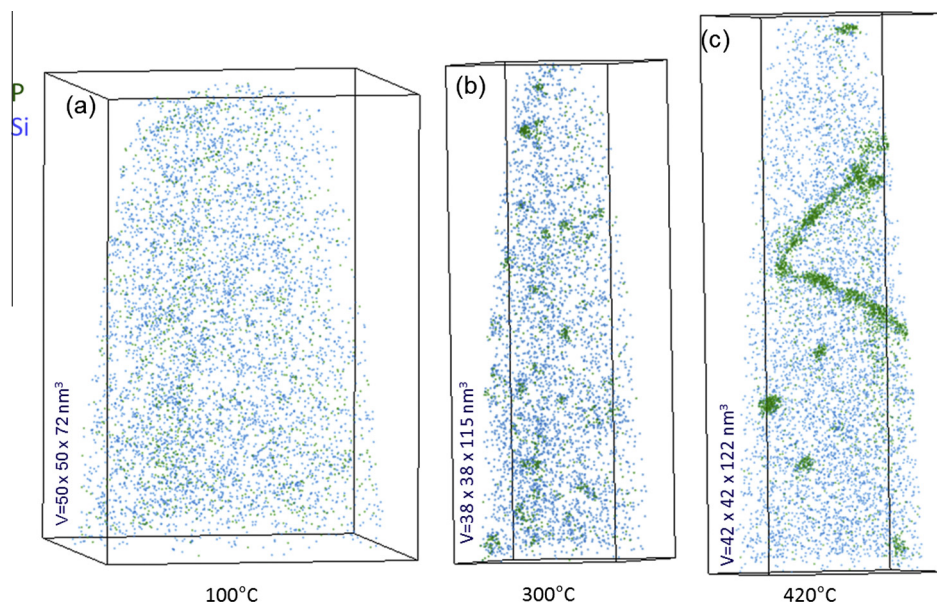


Fig. 1. APT reconstructions of the Fe–9%Cr alloy after ion irradiation at (a) 100 °C, (b) 300 °C and (c) 420 °C. The dose is equal to 0.5 dpa. Blue dots represent Si atoms, green ones, P atoms. Segregation of Si and P evidences the presence of a dislocation line in (c). (For interpretation of the references to colour in this figure legend, the reader is referred to the web version of this article.)

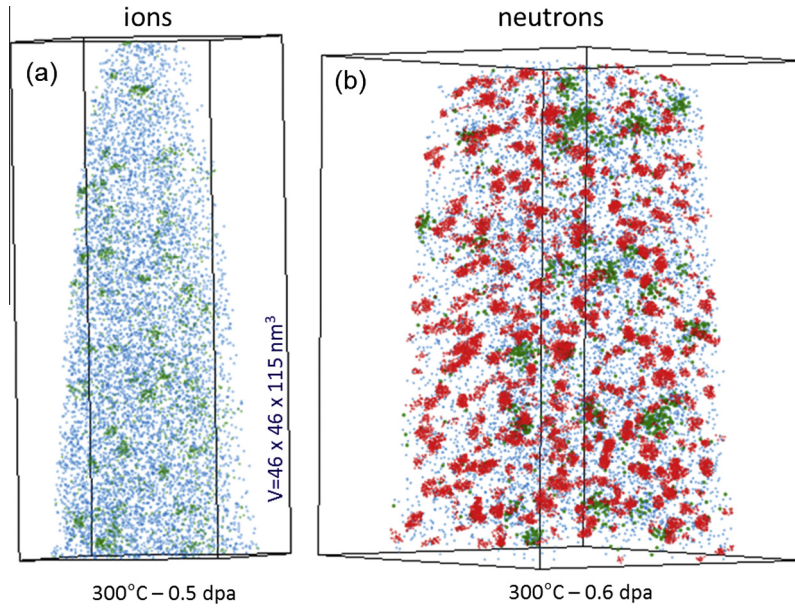


Fig. 2. APT reconstructions of the Fe–12%Cr alloy after (a) ion irradiation at 0.5 dpa and (b) neutron irradiation at 0.6 dpa. Irradiations were performed at 300 °C. Si atoms are in blue, P ones are in green. Red particles correspond to Cr-enriched clusters ($X_{Cr} > 28\%$). (For interpretation of the references to colour in this figure legend, the reader is referred to the web version of this article.)

Table 2
Number density (ND) and size of solute – clusters observed in Fe–9%Cr and Fe–12%Cr at different temperatures after high energy ion irradiation and neutron irradiation at 300 °C [11,14].

	Fe–9at.%Cr		Fe–12at.%Cr	
	300 °C		420 °C	
	Ion irradiation 0.5 dpa	Neutron irradiation 0.6 dpa [11,14]	Ion irradiation 0.5 dpa	Neutron irradiation 0.6 dpa [11,14]
ND (10^{23} m^{-3})	2.8 ± 0.6	2.4 ± 0.5	0.52 ± 0.06	3.3 ± 0.6
Radius (nm)	1.5 ± 0.3	1.65 ± 0.2	1.9 ± 0.2	1.3 ± 0.3

Table 3
Solute enrichment ($\Delta C_i = C_i - C_i^{matrix}$) in at.% measured in solute clusters in Fe–9%Cr and Fe–12%Cr after ion and neutron irradiation at 300 °C at 0.5 and 0.6 dpa respectively. C_i is the mean core composition of the clusters.

Alloy	Fe	Cr	Si	P	Ni
<i>Ions</i>					
Fe–9%Cr	Bal.	5.8 ± 1.6	2.0 ± 0.7	2.4 ± 0.6	0.4 ± 0.4
Fe–12%Cr	Bal.	2.7 ± 1.3	1.3 ± 0.4	3.5 ± 0.7	0.3 ± 0.2
<i>Neutrons [11,14]</i>					
Fe–9%Cr	Bal.	6.7 ± 1.3	6.6 ± 0.8	2.2 ± 0.5	1.3 ± 0.4
Fe–12%Cr	Bal.	16.0 ± 2.4	7.8 ± 1.5	3.3 ± 1.0	1.2 ± 0.6

recombination rate. RIS intensity increases, as we observed after irradiation at 300 and 420 °C. At even higher temperature, the high mobility of point defects induces back-diffusion and then a decrease of the RIS intensity. This part of the bell-curve has not been observed in this work but has been recently evidenced by Wharry and Was [40,41] in F–M steels by measuring enrichment at grain boundaries after proton irradiation. They explored the temperature dependence from 300 °C to 700 °C for a dose rate of 1.2×10^{-5} dpa/s. They observed a maximum of the RIS intensity at about 400–450 °C for Ni, Si and Cr. The position of the maximum is dependent on the dose rate. A shift towards higher temperature is expected for higher dose rate. So it is not possible to directly compare our results to those of Wharry and Was. Nevertheless,

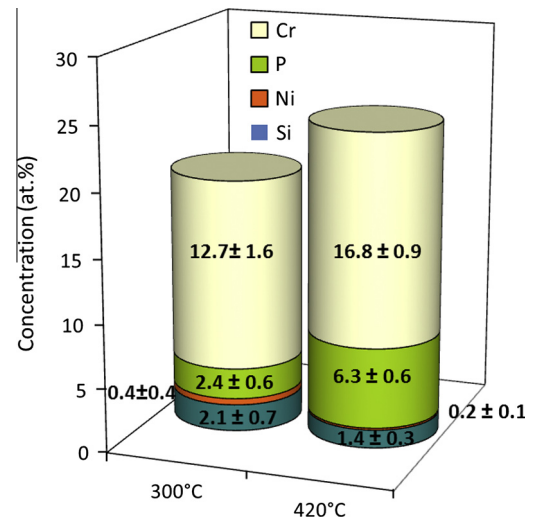


Fig. 3. Composition of the solute clusters (at.%) in Fe–9Cr irradiated at 300 °C and 420 °C up to 0.5 dpa (only solute and impurity concentration are given, Fe concentration is given by the balance).

our results are consistent with their observations for Cr. For Si, the maximum seems to appear at lower temperature in our case but the trend has to be confirmed. For P, it is not possible to compare as there are no data about this specie in [40,41].

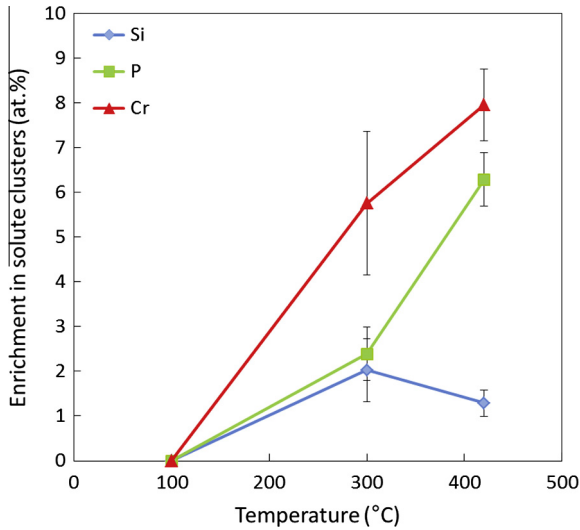


Fig. 4. Evolution of Cr, Si and P enrichment in solute clusters with temperature in Fe-9%Cr irradiated to 0.5 dpa with Fe⁺ ions.

To summarize, the RIS behavior we report confirm the radiation induced origin of the Cr/Si/P/Ni clusters that was assessed in [11,14]. These features are therefore either associated to small point defects clusters and/or to concentration fluctuations acting as traps for interstitials. Indeed, P, Cr and Si are known to have a strong binding with self-interstitials [42–46].

It is not possible to conclude on this point and to distinguish the two processes. However, the results evidence a homogeneous distribution of the point defect sinks at the origin of the formation of the clusters and a positive flux coupling between point defects and solutes (P, Ni, Si and Cr) under the irradiation conditions used here. This is consistent with the RIS behavior observed at dislocation loops in the literature. For example, Jiao et al. [47] observed Si and Ni enrichment in proton irradiated HCM12A and T91. They also observed Cr enrichment at dislocation loops in T91 [47]. Kusenkeno et al. [48] measured Cr enrichments at large dislocation loops in F82H irradiated with high energy protons and spallation neutrons. Nevertheless, as for Cr behavior at grain boundaries, some contrary results are observed at dislocation loops. Indeed, Jiao et al. [47] reported Cr depletion at dislocation loops in proton HCM12A steel irradiated under the same condition than the T91 which show Cr enrichments.

The results are also consistent with the expected diffusion behavior of the different species. Indeed, a positive coupling between P, Si and Ni and points defect fluxes are forecasted. P, Si and Ni are expected to be vacancy-dragged [43,49–52] and P and Ni also diffuse via interstitial mechanism [42,43,45,46,53–56]. Regarding Cr atoms, calculations [41,57] predicted that Cr diffusion is dependent on the relative magnitude of the vacancy and the interstitial diffusion coefficients. Indeed, these two mechanisms leads to opposite trends: enrichment in case of interstitial diffusion and depletion for vacancy diffusion. Under this hypothesis, in the irradiation conditions used here, contribution of Cr interstitial diffusion appears to be the predominant diffusion mechanism.

3.2. Comparison with neutron irradiation

These alloys were also neutron irradiated at 300 °C to 0.6 dpa. α' precipitation was shown to be radiation enhanced [11,12]. Full APT characterization is available in [11,14,30,31].

Fig. 2b displays a 3D reconstruction of the Fe-12%Cr after neutron irradiation. A direct comparison is then possible between ion

and neutron irradiations by comparing Fig. 2a and b which present the chemical distributions observed after ion and neutron irradiation of the Fe-12%Cr at the same temperature and at a similar dose. A striking difference between the two microstructures is that a very high number density ($2 \times 10^{24} \text{ m}^{-3}$ [11,14]) of α' clusters were formed after neutron irradiation. This difference must originate in the dose rate difference: $1.3 \times 10^{-7} \text{ dpa/s}$ for neutron irradiation and $2.2 \times 10^{-4} \text{ dpa/s}$ for ions (3 orders of magnitude higher). Because of this difference in dose rate, samples were ion irradiated during a time about 3 orders of magnitude shorter than samples neutron irradiated at the same dose: 1 h 15 of effective irradiation time (in total 2 h 30 of holding at the irradiation temperature) for ions versus about 55 days for neutrons. Regarding the latter information and the results, this means that, during 2 h 30 of ion irradiation, Cr atoms have not enough time to form the α' particles that are formed during the 55 days of neutron irradiation at 300 °C.

Contrary to α' particles, the solute clusters are present in both cases. Similar clusters were also observed in F82H irradiated at 345 °C with high energy proton and spallation neutrons [48]. Within uncertainties, the number density and radius measured after ion irradiation at 300 °C are similar to the values obtained after neutron irradiation even if one could note a slightly lower radius after ion irradiation (Table 2). The solute enrichments are given in Table 3. After neutron irradiation, the total enrichment is higher than after ion irradiation at the same temperature. The Cr enrichment is similar after neutron and ion irradiation for the Fe-9%Cr but one observes a substantial increase for the Fe-12%Cr under neutron irradiation. This reveals a strong dependence with the Cr bulk composition of Cr RIS under neutron irradiation as already pointed out in a previous work [11]. The fact that this dependence was not observed under ion irradiation is probably also a manifestation of the flux effect.

Ni and Si segregation intensity also appear to be dose rate dependent. Under neutron (low dose rate) the enrichment is much higher than under ion irradiation (high dose rate). Regarding P enrichment, results suggest that there is no dose rate dependence for this impurity as a similar concentration is reported under ion and neutron irradiation. However, this could be due the bell-shaped evolution of RIS with temperature and the shift of the curve towards lower temperatures for lower dose rate (neutron irradiation). In that case, RIS intensity of P measured under neutron irradiation would belong to the downward part of the bell-shaped curve whereas it is situated in the upward part under ion irradiation (see part 3.1). Of course, it is not possible to conclude here as these comparisons are made only between two dose rates and at one temperature.

Another point that is relevant to focus on is that solute clusters are richer in P than in Si after ion irradiation whereas it is the inverse after neutron irradiation. Considering the irradiation time difference between the two irradiation kinds, this would suggest that P enriched first the solute clusters. This is coherent with diffusion data (migration energy of P mixed-dumbbells is the lowest one [42,56–58]) and with the strong affinity of P with self-interstitials. Indeed, experimental results of Hardouin-Duparc [59] highlighted the link between P and the increase in the number density of dislocation loops in electron irradiated Fe-P. Also, ab initio calculations [42,43] evidenced the formation of very stable and immobile complexes between P atoms and interstitials. According to these calculations, the complexes could be stable nuclei of dislocation loops. It is also relevant to note that Cr and Si also trap the interstitials [55] and could also participate to the stabilization of point defects clusters. But as the diffusion coefficient of these species is much lower than the P's one, it appears reasonable to consider that P atoms first stabilize point defect clusters and then followed by Ni, Si and Cr enrichments.

4. Conclusion

In this paper, we presented the atomic scale investigation of the microstructure of two Fe–Cr alloys (Fe–9%Cr and Fe–12%Cr of low purity) that were irradiated with Fe⁺ ions at 100 °C, 300 °C and 420 °C at 0.5 dpa. Results were compared to data obtained in the same alloys neutron irradiated at 300 °C up to 0.6 dpa [11].

Irradiation of these alloys of low purity induces formation of two families of clusters: solute clusters enriched in Cr, P, Si and Ni and α' particles. However, no α' precipitates were formed under the ion irradiation conditions used in this work whereas they appeared under neutron irradiation. Even if α' precipitation is enhanced, the irradiation time was too short or the dose rate was too high to enable α' particles to appear under the ion irradiation. As under neutron irradiation, after ion irradiation there is formation of Cr/Si/P/Ni clusters that are homogeneously distributed for temperature higher than 300 °C. These clusters are shown to be radiation induced segregations that are associated to homogeneously distributed point defect sinks. Comparison of the cluster composition after ion irradiation and neutron irradiation, suggests that P atoms could play an important role in the appearance of the solute clusters by stabilizing point defect clusters that could later be enriched in Ni, Si and Cr.

Acknowledgment

Part of this work was supported by the European Commission within the project GETMAT under grant agreement FP7-212175 and by GEDEPEON (Groupement National de recherche CEA-CNRS-EDF-AREVA). This work also contributes to the Joint Programme on Nuclear Materials (JPNM) of the European Energy Research Alliance (EERA). The authors gratefully acknowledge B. Radiguet for useful discussions.

References

- [1] F. Garner, M. Toloczko, B. Sencer, *J. Nucl. Mater.* 276 (2000) 123.
- [2] R.L. Klueh, D.R. Harries, *ASTM* (2001).
- [3] P. Dubuisson, D. Gilbon, J.L. S eran, *J. Nucl. Mater.* 205 (1993) 178.
- [4] J.J. Kai, R.L. Klueh, *J. Nucl. Mater.* 230 (1996) 116.
- [5] D.S. Gelles, L.E. Thomas, *Ferritic Alloys for Use in Nuclear Energy Technologies*, TMS-AIME, Warrendale, PA, 1984, p. 559.
- [6] P. Maziasz, *J. Nucl. Mater.* 169 (1989) 95.
- [7] T.S. Morgan, E.A. Little, R.G. Faulkner, *Effect of radiation on materials*, in: R.E. Stoller, A.S. Kumar, D.S. Gelles (Eds.), *16th International Symposium, ASTM STP 1175* (1994) 607.
- [8] Z. Jiao, G.S. Was, *J. Nucl. Mater.* 425 (2012) 105.
- [9] Z. Jiao, V. Shankar, G.S. Was, *J. Nucl. Mater.* 419 (2011) 52.
- [10] C. Fazio, D. Gomez Briceno, M. Rieth, A. Gessi, J. Henry, L. Malerba, *Nucl. Eng. Des.* 241 (2011) 3514.
- [11] V. Kuksenko, C. Pareige, P. Pareige, *J. Nucl. Mater.* 432 (2013) 160.
- [12] F. Bergner, A. Ulbricht, C. Heintze, *Scr. Mater.* 61 (2009) 1060.
- [13] M. Bachhav, G. Robert Odette, E.A. Marquis, *Scr. Mater.* 74 (2014) 48.
- [14] V. Kuksenko, C. Pareige, C. G enevois, F. Cuvilly, M. Roussel, P. Pareige, *J. Nucl. Mater.* 415 (2011) 61.
- [15] B. Radiguet, A. Barbu, P. Pareige, *J. Nucl. Mater.* 360 (2007) 104.
- [16] P. Pareige, B. Radiguet, A. Barbu, *J. Nucl. Mater.* 352 (2006) 75.
- [17] E. Meslin, B. Radiguet, P. Pareige, A. Barbu, *J. Nucl. Mater.* 399 (2010) 137.
- [18] M. Matijasevic, A. Almazouzi, *J. Nucl. Mater.* 377 (2008) 147.
- [19] M. Matijasevic, *Microstructure and Mechanical Properties of Fe–Cr Model Alloys and High Cr Steels under Neutron Irradiation*, Gent University, Belgium, 2007.
- [20] Generation IV and Transmutation Materials (GETMAT) – Collaborative Project, Seventh European Commission Framework Programme, Fission – 6.0.02 – Cross Cutting Topic: Materials for Transmutation Technologies and Advanced Reactors FP7-212175, 2007.
- [21] J.F. Ziegler, M.D. Ziegler, J.P. Biersack, *Nucl. Instrum. Meth. Phys. Res. Sect. B* 268 (2010) 1818.
- [22] J.F. Ziegler, J.P. Biersack, U. Littmark, *The Stopping and Range of Ions in Matter*, Pergamon Press, 1985.
- [23] ASTM E521, *Standard Practice for Neutron Radiation Damage Simulation by Charged-Particle Irradiation*, Annual Book of ASTM Standards, vol. 20.02, ASTM International, West Conshohocken, PA, 2009.
- [24] R.E. Stoller, M.B. Toloczko, G.S. Was, A.G. Certain, S. Dwaraknath, F.A. Garner, *Nucl. Inst. Meth. Phys. Res. Sect. B* 310 (2013) 75.
- [25] M.J. Norgett, M.T. Robinson, I.M. Torrens, *Nucl. Eng. Des.* 33 (1975) 50.
- [26] C. Heintze, F. Bergner, A. Ulbricht, H. Eckerlebe, *J. Nucl. Mater.* 409 (2011) 106.
- [27] F. Bergner, C. Pareige, V. Kuksenko, L. Malerba, P. Pareige, A. Ulbricht, A. Wagner, *J. Nucl. Mater.* 442 (2013) 463.
- [28] M. Lambrecht, L. Malerba, *Acta Mater.* 59 (2011) 6547.
- [29] C. Heintze, F. Bergner, M. Hern andez-Mayoral, *J. Nucl. Mater.* 417 (2011) 980.
- [30] V. Kuksenko, C. Pareige, C. Genevois, P. Pareige, *J. Nucl. Mater.* 434 (2013) 49.
- [31] V. Kuksenko, C. Pareige, P. Pareige, *J. Nucl. Mater.* 425 (2012) 125.
- [32] G. Da Costa, F. Vurpillot, A. Bostel, M. Bouet, B. Deconihout, *Rev. Sci. Instrum.* 76 (2005) 013304.
- [33] E. Bemont, A. Bostel, M. Bouet, G. Da Costa, S. Chambrelaud, K. Hono, B. Deconihout, *Ultramicroscopy* 95 (2003) 231.
- [34] D. Blavette, B. Deconihout, A. Bostel, J.-M. Sarrau, M. Bouet, A. Menand, *Rev. Sci. Instrum.* 64 (1993) 2911.
- [35] B. Gault, M.P. Moody, J.M. Cairney, S.P. Ringer, *Springer Ser. Mater. Sci.* 160 (2011).
- [36] M. Miller, *Atom Probe Tomography*, Kluwer Academic/Plenum Publishers, New York, 2000.
- [37] E. Meslin, B. Radiguet, M. Loyer-Prost, *Acta Mater.* 61 (2013) 6246.
- [38] V. Kuksenko, *Model Oriented Irradiation Experiments in Fe–Cr Model Alloys*, PhD., University of Rouen, France, 2011.
- [39] M. Hernandez-Mayoral, L. Malerba, M. Lambrecht, V. Kuksenko, C. Pareige, P. Pareige, F. Bergner, C. Heintze, A. Ulbricht, T. Toyama, M. Ramesh, B. Minov, M. Konstantinovi c, *GETMAT (FP7-212175) Deliverable D4.7* (2013).
- [40] J.P. Wharry, G.S. Was, *J. Nucl. Mater.* 442 (2013) 7.
- [41] J.P. Wharry, G.S. Was, *Acta Mater.* 65 (2014) 42.
- [42] E. Meslin, C.-C. Fu, A. Barbu, F. Gao, F. Willaime, *Phys. Rev. B* 75 (2007) 094303.
- [43] C. Domain, C.S. Becquart, *Phys. Rev. B* 71 (2005) 214109.
- [44] D. Terentyev, P. Olsson, T.P.C. Klaver, L. Malerba, *Comput. Mater. Sci.* 43 (2008) 1183.
- [45] E. Vincent, C.S. Becquart, C. Domain, *J. Nucl. Mater.* 359 (2006) 227.
- [46] F. Maury, A. Lucasson, P. Lucasson, P. Moser, Y. Loreaux, *J. Phys. F – Met. Phys.* 15 (1985) 1465.
- [47] Z. Jiao, G.S. Was, *Acta Mater.* 59 (2011) 4467.
- [48] V. Kuksenko, C. Pareige, P. Pareige, Y. Dai, *J. Nucl. Mater.* 447 (2014) 189.
- [49] L. Messina, Z. Chang, P. Olsson, *Nucl. Inst. Meth. Phys. Res. Sect. B* 303 (2013) 28.
- [50] L. Messina, Z. Chang, P. Olsson, *Private communication* (n.d.).
- [51] Y. Nagai, K. Takadate, Z. Tang, H. Ohkubo, H. Sunaga, H. Takizawa, M. Hasegawa, *Phys. Rev. B* 67 (2003) 224202.
- [52] A.V. Barashev, *Philos. Mag.* 85 (2005) 1539.
- [53] F. Maury, P. Lucasson, A. Lucasson, F. Faudot, J. Bigot, *J. Phys. F* 17 (1987) 1143.
- [54] F. Maury, A. Lucasson, P. Lucasson, Y. Loreaux, P. Moser, *J. Phys. F* 16 (1986) 523.
- [55] J. Wallenius, P. Olsson, L. Malerba, D. Terentyev, *Nucl. Inst. Meth. Phys. Res. Sect. B* 255 (2007) 68.
- [56] H. Abe, E. Kuramoto, *J. Nucl. Mater.* 271 (1999) 209.
- [57] S. Choudhury, L. Barnard, J.D. Tucker, T.R. Allen, B.D. Wirth, M. Asta, D. Morgan, *J. Nucl. Mater.* 411 (2011) 1.
- [58] P. Olsson, *J. Nucl. Mater.* 386–388 (2009) 86.
- [59] A. Hardouin-Duparc, *Etude de La Formation Sous Irradiation Des Amas de D efauts Ponctuels Dans Les Alliages Ferritiques Faiblement Alli s*, PhD thesis, Paris XI-Orsay University, 1998.